
A Spring Assisted One Degree of Freedom Climbing Model

J.E. Clark¹ and D.E. Koditschek²

¹ University of Pennsylvania, Philadelphia, PA, USA
jonclark@grasp.upenn.edu

² University of Pennsylvania, Philadelphia, PA, USA
kod@ese.upenn.edu

Summary. A dynamic model of running—the spring-loaded inverted pendulum (SLIP)—has proven effective in describing the force patterns found in a wide variety of animals and in designing and constructing a number of terrestrial running robots. Climbing or vertical locomotion has, on the other hand, lacked such a simple and powerful model. Climbing robots to date have all been quasi-static in their operation. This paper introduces a one degree of freedom model of a climbing robot used to investigate the power constraints involved with climbing in a dynamic manner. Particular attention is paid to understanding how springs and body dynamics can be exploited to help relieve a limited power/weight ratio and achieve dynamic running and climbing.

1 Introduction

We seek a fast and agile robot that can traverse both vertical and horizontal real world terrain. Dynamic locomotion over unstructured and natural terrain has proven to be a difficult task. A large number of walking robots have been built, but only recently have running robots been developed that can move at speeds of bodylengths/second over rough terrain [6, 21, 15]. The *Rhex* [6] and *Sprawl* [15] families of dynamic machines are based on a Spring-loaded Inverted Pendulum (SLIP) model of running developed from biomechanical research [13, 20]. They have simple morphologies with only one actuator per leg, are polypedal, run mostly open-loop, and rely on springs in the legs to passively self-stabilize.

On the other hand, there have only been a few legged robots that can climb vertical surfaces, and they have generally been limited to quasi-static climbing regimes. Their reliance on vacuum or magnetics to achieve the adhesive forces necessary for vertical climbing has limited them to select man-made surfaces such as glass and metal [19, 10, 23]. Recently foot-hold based [11, 12] and vectored thrust based climbers [1] have been developed, but they only

slightly extend the range of traversable surfaces and do not address the role of dynamics in climbing.

The motivation for this work is the ongoing development of the *RiSE* robot—a bio-inspired hexapedal platform that is intended to both run and climb vertical surfaces [8]. Currently under development are micro-spine [7, 16] and dry-adhesive feet [22] to allow attachment to a wide range of natural vertical environments. The current instantiation of the robot, however, is otherwise like the remainder of climbing robots in that it moves slowly and its control is based on quasi-static assumptions. The purpose of this work is to explore how to achieve dynamic climbing and how that can be used to improve the performance of the RiSE climbing robot.

To this end we discuss some of the fundamental differences between dynamic running and climbing and introduce a simple one-dimensional dynamic climbing model to investigate approaches to mitigate some of the difficulties in achieving dynamic climbing.

1.1 Dynamic Climbing

We reserve the term *dynamic* for robots that manage their kinetic as well as their potential energy. For example, dynamic level ground running can be distinguished from quasi-static locomotion by the phasing of kinetic and gravitational potential energy during a stride. Generally, dynamic runners are distinguished in physical structure by their essential use of springs in the legs. These leg springs act as reservoirs that can store and return energy at whatever required rate. In a typical dynamic gait, the spring energy is collected during the initial phase of a stride (“compression”) and returned during the second phase (“decompression”) as work done against gravity needed to raise again the center of mass back close to its height lost in the initial phase. Dynamic runners can (but need not) adopt an aerial phase gait to buy time for leg recirculation, thereby affording speeds that surpass the inevitable frequency limits of their leg swing actuators. In such situations, springs can recover and return the kinetic energy otherwise lost in body deceleration.

Properly arranging these exchanges of kinetic and spring and gravitational energy requires control schemes designed to do more than simply track the joint reference trajectories typically used by walkers. The resulting dynamic stability confers a degree of agility and maneuverability impossible to achieve in quasi-static walking gaits. The question arises whether spring assistance can be introduced in climbing that yields analogous benefits.

The major difference between climbing and running is in the alignment of the gravity vector with respect to the direction of travel. We suggest that this has three primary impacts on legged climbers. The first is that travel aligned with the gravity vector implies that any forward progression increases the gravitational potential of the robot, resulting in a net drain on the rest of the system’s energy. As a consequence the SLIP model, which relies on

the interchange of kinetic and gravitational potential energy from hopping or bouncing to regulate the energy during a stride, no longer applies.

In addition to necessarily changing the way in which kinetic and spring potential energy are exchanged with gravitational potential energy, a vertical heading also implies that ground impacts are not induced by gravity. Especially for the front feet ground contact must be actively generated. This changes, and to some degree reduces, the role of springs in mitigating ground contact forces. Successful running robots have required springs to regulate the impact at ground contact, and this is not necessarily the case for climbers.

A third major difference for climbing robots is the necessity of bi-lateral or “adhesive” foot constraints. The development of feet that create an in-pulling force to the wall is one of the major design requirements in a climbing robot. Having to create feet that grasp the wall to deal with the inherent pitch instability serendipitously reduces the chance of tipping in the roll direction—which is a major source of instability in level ground runners. Once attached, tipping becomes less of a problem, but motions such as repositioning the feet on the ground via sliding, as is often done in turning, become more difficult.

In some sense these differences make climbing easier than running since severe foot impacts and lateral tipping are less likely to occur. On the other hand getting good foot attachment and regulating the system’s energy become much more difficult. The problem of attachment has and continues to receive a fair amount of attention. The second problem, more effectively using the system’s power resources, motivates our investigation with a simple dynamic climbing model.

A dynamic robot may lend scansorial machines advantages relative to today’s quasi-static climbers analogous to the superiority of level ground runners over their quasi-static walking counterparts: simplified control; improved efficiency; access to and mobility through otherwise impassible terrain obstacles; and, of course, faster speeds.

1.2 Power and Speed Constraints

We propose a simple one-dimensional climbing model to investigate the power requirements and constraints associated with dynamic behavior. As a target for dynamic motion we set a stride frequency of 3.5 Hz for our 3 kg robot. Specifically, this figure is associated with the natural frequency of the linear mass spring model associated with purely vertical SLIP hopping.

At lower frequencies, back-of-the-envelope calculations developed in Appendix A1 suggest that spring-extension requirements for SLIP-like running (i.e., resonant bouncing in the sagittal plane over level ground) would incur impractically long leg compression.

Another method that has been used to characterize the onset of running is the Froude number, (v^2/gl) , where v is the average fore-aft running speed, l is the leg length and g is the constant of gravitational acceleration. The Froude number is a dimensionless constant that has been used in biomechanics to

predict the dynamic similarity in legged animals that is manifest over a wide range of sizes. It has been shown that many animals prefer to switch from a walk to a run at speeds where their Froude number is about 0.5 [4, 18].

RiSE climbing at the target frequency of 3.5 Hz would travel at 0.55 m/s which corresponds to a Froude number of 0.2. While it is not clear that the Froude number is as applicable to climbing as it is to terrestrial locomotion, it does give some indication of when velocity begins to significantly affect the energetics of motion. The relatively low value of our target frequency's Froude number with respect to observed animal gait transitions suggests that the target frequency we have chosen for dynamic climbing is probably not too high.

With the current trajectory-tracking, quasi-static control scheme the robot can climb with a stride frequency of 0.5 Hz. Is it theoretically possible to achieve the required 7x increase in speed without changing the motors or decreasing the robot's mass?

The current robot, weighing 3 kg and equipped with two 4.5 W rated servo motors for each of its six legs, has an input electrical power-to-mass ratio of 18:1. In order to climb vertically at our dynamic threshold (0.53 m/s with a stride length of 0.15 m) requires a mechanical output power of 16 W just to deliver the energy expended to increase the system's gravitational potential.

Experiments on Geckos running up vertical walls has shown that the mechanical power that they expend to run at speeds up to 10 bodylengths/second is about 5 W per kilogram of animal [9]—about the same ratio as for RiSE were it to run at 3.5 Hz. What is remarkable is that for the gecko the mechanical power expended when climbing is only about 10% greater than the amount of energy lost to gravitational potential.

The 16 W power requirement for RiSE running at this speed represents 30% of the maximum continuous electrical input power that the robot motor's can consume without thermal damage. In reality only a small percentage of the motors' 54 W rating will be converted into useful mechanical work. The two major reasons for this are (1) the motors are run at maximum power for only a small segment of the stride and (2) motor inefficiencies (e.g. thermal losses in the windings and mechanical losses in the bearings) and system "drag" (e.g., transmission losses, generation of internal forces and negative work associated with securing footholds) significantly diminish the mechanically useful component of the power the motors consume.

In this paper we address the first of these two problems. Specifically we consider how to use dynamic gaits and body/leg springs to better utilize the available motor power. We show that in the ideal case these approaches significantly reduce the peak power demanded from the motors permitting a smaller gear reduction, which in turn allows a higher stride frequency.

With ideal motors the changing demands for torque and speed during the leg cycle could be met by implementing a torque control law and allowing the motor to operate at different points along the speed-torque curve. As shown in Fig. 2 for the current motors, only 20% of the torque range is available for

continuous use. This dramatically reduces the flexibility of any such motor control law. Instead we investigate how to use passive springs and the body's inertia to maximize the application of the available electrical power.

The remainder of this paper is organized as follows. Section 2 describes the one-dimensional model of climbing that we use to evaluate the efficacy of the proposed schemes. The simplifying assumptions and equations of motion are given. Section 3 details the numerical studies undertaken and compares the various cases considered. Section 4 reviews the results and gives some areas of future work.

2 Model Description

2.1 Assumptions

The RiSE robot (see Fig. 1a) is a six limbed climber with two controlled degrees of freedom per leg. Each leg can rotate about an axis parallel to the direction of motion, lifting the foot away from the ground (wing DOF). The second actuated degree of freedom controls the rotation of the crank segment of a four bar mechanism connecting the foot to the body. The foot is attached to the follower link of the mechanism and traces a roughly elliptical path (see Fig. 3) in a plane passing through the line of action of the wing DOF.

With the assumption that the wing DOF is primarily used to specify the point of touchdown and lift-off in the cycle, the motion of the legs and body can be modeled as planar. This abstraction neglects, among other things, body pitch away from the wall—which is known to be a significant issue.

The further assumptions that the robot uses an alternating tripod gait and that lateral motions of the robot are of secondary importance allow the

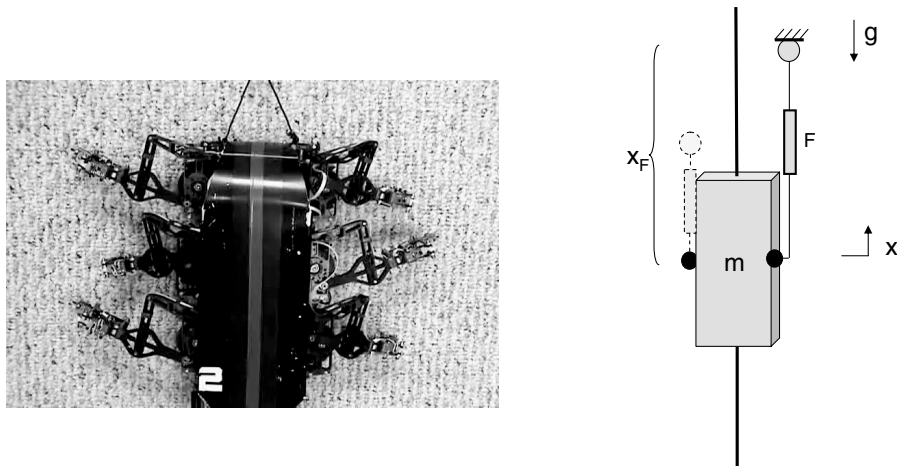


Fig. 1. (A) Picture of RiSE climbing and (B) schematic of the simple climbing model

construction of a single degree of freedom model of climbing, shown in Fig. 1b. The model consists of a point mass body with two virtual, massless legs. The extension of the foot (X_F) during stance is fixed by the leg kinematics. In this very simple model, we are ignoring friction from the legs, foot slipping, etc. Although this oversimplification of the system ignores many real and important effects, it is hopefully sufficient to examine some basic power and stability issues and provide a basis for future examinations.

2.2 Stance Dynamics

The sum of the forces in the vertical direction is given by:

$$m\ddot{x} = F - mg \quad (1)$$

where m is the mass of the body, F is the force generated by the motor, and g is the gravitational constant opposing the motion.

The force generated by the leg actuator is based on a very simple motor model. Due to thermal concerns arising from the nearly continuous use of the motors when climbing, we assume that the motors operate within their recommended operating range, shown in Fig. 2. Although the stall torque of the motor is 28.8 mNm , the continuous operational limit (τ_{Max}) is only 4.98 mNm . This represents about 20% of the speed/torque curve given by:

$$\tau = \frac{\omega - \omega_{nl}}{-k_m}$$

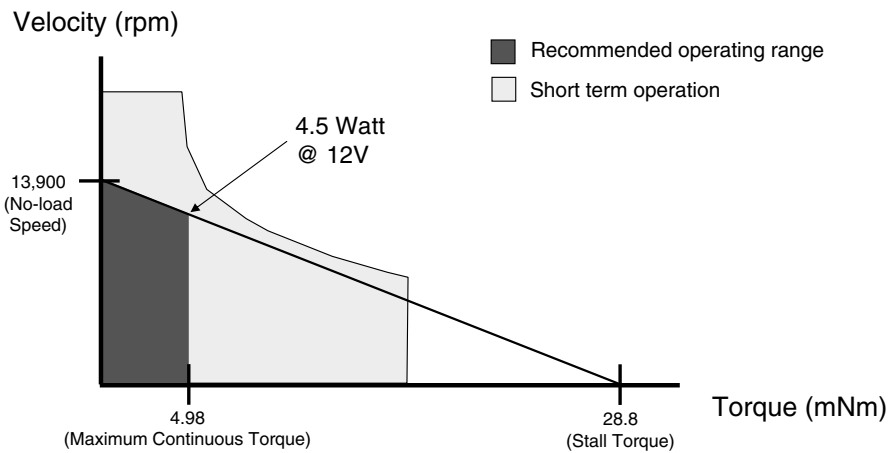


Fig. 2. Model and specifications for the motors used on the *RiSE* robot. Data from Maxon Precision Motors Inc. RE-16 motor (16 mm diameter, graphite brushes, 4.5 Watt, part number 118730) [2]

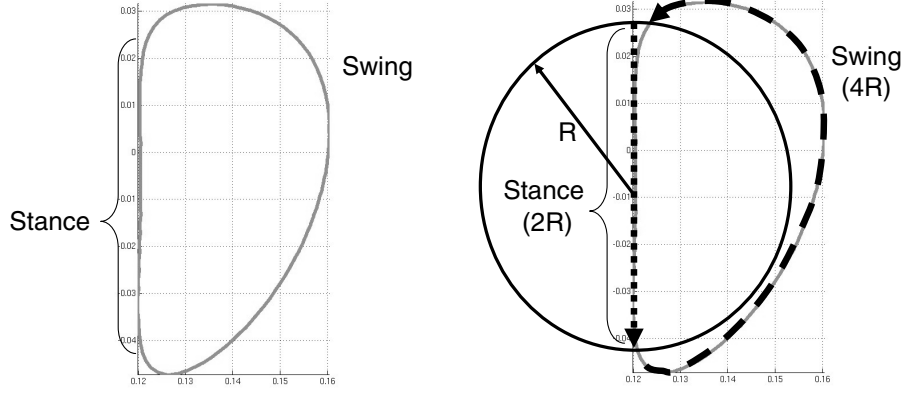


Fig. 3. Nominal RiSE foot trajectory and simplification used in the model. The RiSE leg kinematics result in a swing phase that is almost twice as long as the stance phase. (Leg trajectory from RISE [8])

where ω is the angular velocity of the motor, ω_{nl} is the no-load velocity limit, and k_m is the slope of the speed/torque curve. Thus the maximum continuously available torque is given by:

$$\tau = \min \left(\frac{\omega - \omega_{nl}}{-k_m}, \tau_{Max} \right)$$

In order to adapt to a one DOF linear model the trajectory of the four-bar traveler is approximated with a circle of radius R , as shown in Fig. 3.

Linear Coordinates

With the following conversions:

$$F_{Max} = \frac{\tau_{Max}}{R}$$

$$\dot{x}_{nl} = R \omega_{nl}$$

$$k_e = \frac{\dot{x}_{nl}}{F_{Max}} = \frac{R^2 \omega_{nl}}{\tau_{Max}} = R^2 k_m$$

the motor torque law becomes:

$$F = \min \left(\frac{\dot{x} - \dot{x}_{nl}}{-k_e}, F_{Max} \right)$$

where (k_m) is the slope of the force/velocity curve. With the addition of a gear reduction (G), the force from the motor (F) becomes:

$$F = \min \left(\frac{\dot{x} - \frac{\dot{x}_{nl}}{G}}{-G^2 k_e}, GF_{Max} \right) = \min \left(\frac{G^2 \dot{x} - G \dot{x}_{nl}}{-k_e}, GF_{Max} \right) \quad (2)$$

Combining (1) and (2) yields:

$$\ddot{x} = \frac{1}{m} \left(\min \left(\frac{G^2 \dot{x} - G \dot{x}_{nl}}{-k_e}, GF_{Max} \right) - mg \right) \quad (3)$$

Gait transitions occur when $(X_F - x) = 0$, i.e. when the leg has reached the end of the vertical section of travel. Since the four-bar mechanism fixes the gait trajectory, X_F is fixed at $2R$. Whether the leg is capable of resetting within the duration of the last stance phase is a function of the swing dynamics, described below.

2.3 Massless Swing Dynamics

Of course in the physical system the mass of the legs is non-zero, and the leg's trajectory during the swing phase is a function of its dynamics. Initially, however, these dynamics are ignored and the swing phases is considered as a binary state: either the leg can return to the touchdown position in time, or it cannot.

The time that it will take the leg to retract, t_{Swing} , is bounded by no-load, \dot{x}_{nl} , and max continuous velocity, $\dot{x}_{\tau_{Max}}$, of the foot, as given below:

$$\frac{G \ 2R}{\dot{x}_{\tau_{Max}}} \geq t_{Swing} \geq \frac{G \ 2R}{\dot{x}_{nl}} \quad (4)$$

The left side of 4 represents an upper bound on the duration of the swing phase.

3 Numerical Simulation

3.1 Trajectory vs. Force Based Gaits

In the current control philosophy a gait is generated by specifying a desired trajectory for the path of the feet. Typically four phases are specified: swing, attachment, stance, and detachment. Using the motor encoder readings and PD control the legs attempt to track this trajectory throughout the stride. Forces are generated when errors in the tracking occur. These generally correspond to contact with the ground during attachment, lifting the robot in the face of gravity during stance, and the inertial resistance to the rapid acceleration during swing. Figure 4 shows an idealized trajectory and the corresponding torques generated by the motors. The figure on the left is a projection of foot trajectory in the wing plane. A trace of the wing angle with respect to time is shown on the bottom right. In the plot on the right the solid horizontal

line represents the maximum continuous torque as specified by the motor’s manufacturer. The dotted line is the motor’s mean torque over a stride. The motor torque curve itself is an abstraction of reality where the large spike in the torque graph corresponds to the body acceleration of the foot during stance, and the smaller spike to the acceleration of the foot during swing.

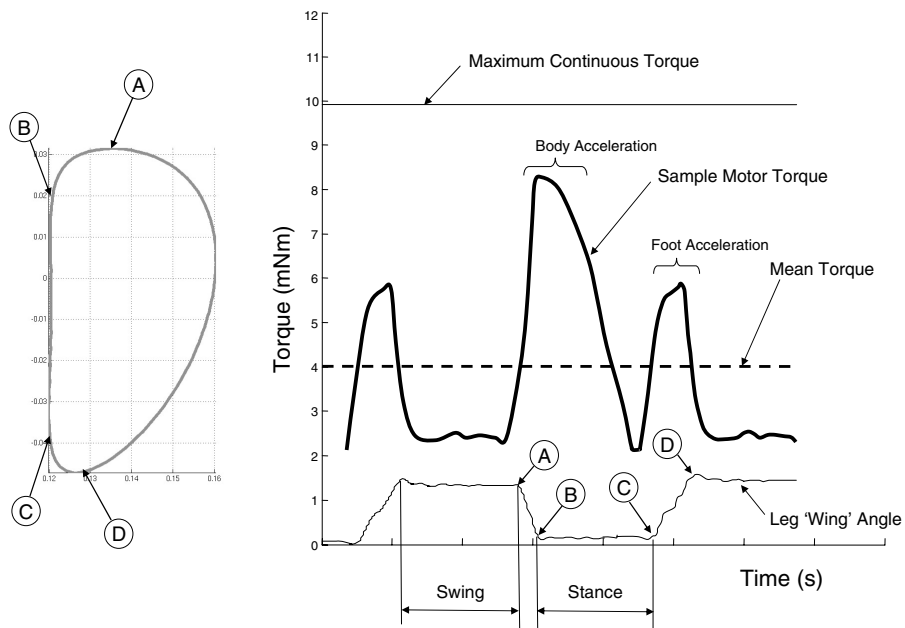


Fig. 4. Sample leg trajectory projected onto the “wing” plane (*left*) and in terms of the wing angle (*right, bottom*). These are used to contextualize the idealized force pattern (*right, top*). The leg trajectory and mean torque plots are based on RiSE robot data [3]

It should be noted that current gaits are designed for effective attachment and detachment rather than optimizing speed or utilization of available motor power. Significant improvements in terms of speed can (and are being) made by refining the shape of the target trajectory—especially during stance and swing—such that the torque demands more closely match the abstraction shown in Fig. 4.

Due to the large gear reduction employed, the ability to shape the torque trajectory is limited. If the peak load on the motors was decreased or distributed more efficiently throughout the stride then the gearing could be reduced and the top speed dramatically increased.

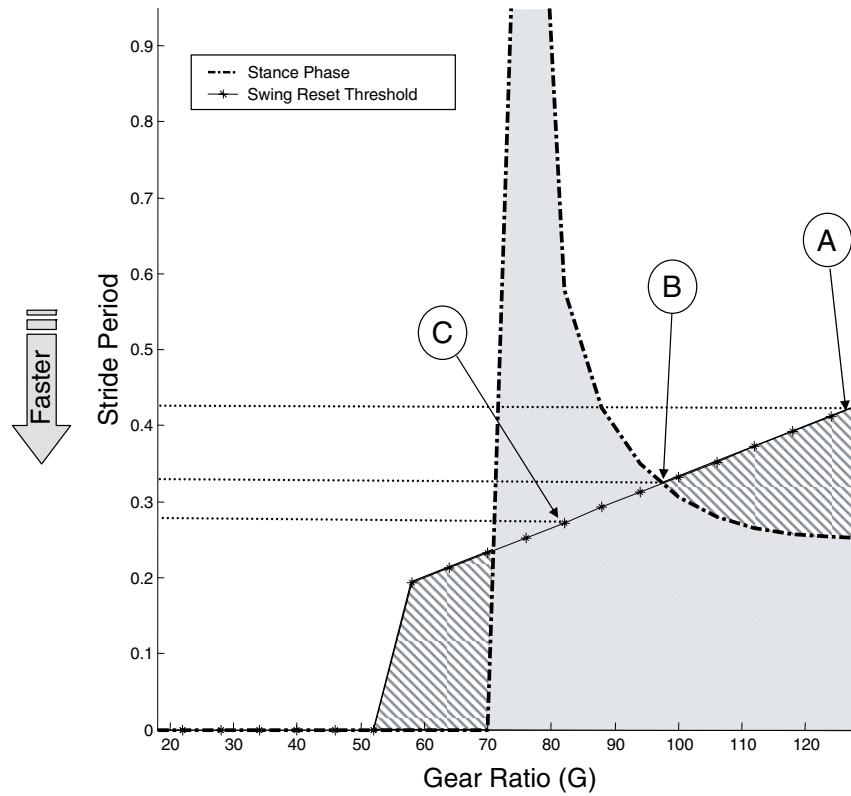


Fig. 5. Simulation results for the base model, showing the minimum possible stride period (maximum speed) for various gear ratios (G). The *shaded areas* under the curves represent regions that are inadmissible as they invalidate either swing or stance phase constraints

Simulation Results

Figure 5 shows how the theoretical minimum stride frequency for the simple model described in Sect. 2.2 varies as a function of gear ratio, G . Since each leg has a kinematically fixed stride length, the stride period is inversely proportional to velocity. The dashed curved line represents the stance phase speed limit for each gear ratio, G . The sloping starred line represents the swing phase reset threshold. Point (A) shows the theoretical maximum speed with the RiSE v1.0 gear ratio. At this gear ratio any higher speeds would require the leg to complete the swing phase faster than the motor can handle. Below a certain gear ratio (point (C) in Fig. 5) the robot no longer has enough force to overcome gravity and cannot climb. Increasing the gear ratio reduces the overall available speed and above a threshold, point (B), the duration of the swing phase becomes the limiting factor.

Point (B) is therefore the theoretical upper bounds on the velocity of the robot using the current trajectory-based gait formulation. This stride frequency (and speed) will, of course, never actually be reached due to the non-instantaneous, and non-trivial, attachment and detachment requirements. Nevertheless it is clear that without some change to the energetics and actuation scheme of the robot it will never be able to reach our target dynamic threshold.

Momentum

If, however, non-zero attachment speeds and the momentum of the body of the robot is explicitly considered in the control scheme the robot could accelerate from one stride to another and higher “steady-state” velocities are possible. This requires either allowing the foot trajectories to change as a function of body velocity or the adoption of some sort of force-based control scheme as is done in our simple model. In either case the new maximum speed will be limited by the swing phase reset time. In this case the fastest configuration corresponds to the lowest gear ratio that will actually lift the robot, as shown by point (C) in Fig. 5.

A potential difficulty with this approach is ensuring that the foot attachment trajectory remains viable as the body velocity increases. This problem is being considered in ongoing work on foot attachment dynamics.

3.2 Spring-Assisted Climbing

An alternative method for increasing speeds with a limited power budget is by the intelligent use of springs to redistribute the cyclic loading and level out the demands on the motors. By lowering the peak force requirements the drive-train gear ratio can be reduced to speed up the overall motion of the robot. This also brings the mean loading on the motors closer to the maximum continuous operation level. Since these motors get the most power at 1/2 of stall, and they are limited to 20% stall by the thermal constraints, maximum achievable power coincides with the maximum continuous operation point.

In this section we consider two approaches to using springs to assist the motion of the body in climbing. The first approach stores energy from the end of the stance phase when the body is decelerating in preparation for attachment and then releases it at the beginning of the next stance phase to help re-accelerate the body. The second approach uses the motor to store energy in a spring during the swing phase, which is then released to assist lifting the body during stance.

3.3 Stance-Stance Transfer

The inspiration and physical motivation for this approach came from observing fast climbing animals such as the gecko which swing their tails and flex

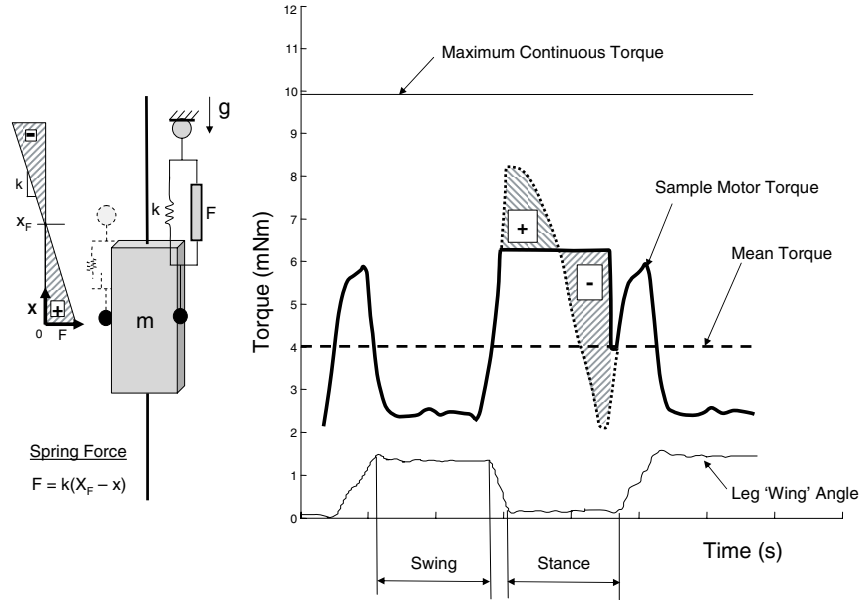


Fig. 6. Schematic of model with body spring and the effect of the spring on the nominal torque profile. The “+” region represents when the spring is assisting the motor, and the “-” region represents when the motor is stretching the spring. (As before, the leg trajectory and mean torque plots are based on RiSE robot data [3])

their backs as they run. One advantage of these motions may be that they shift the phasing of the power distribution to the beginning of a stride when it is needed most to accelerate a body after slowing for foot contact. A proper model for this behavior would include multiple bodies and degrees of freedom. Here we hypothesize that at least part of the effect of these motions can be captured by the linear body spring as shown in Fig. 6. The spring is loaded during the end of the stance phase as the robot slows for attachment and then is released at the beginning of the next stride to assist with the re-acceleration of the body.

The net effect of this body/tail spring is to lower the peak torque spike during stance. This in turn allows us to further change the gear ratio, reducing the maximum continuous torque limit and increasing the stride frequency. With the addition of this spring the equation of motion for the body during stance becomes:

$$\ddot{x} = \frac{1}{m} \left(\min \left(\frac{G^2 \dot{x} - G \dot{x}_{nl}}{-k_e}, GF_{Max} \right) + k(X_F - x) - mg \right) \quad (5)$$

where X_F , the rest length of the spring, is located at the midpoint of stance.

The maximum stiffness of the virtual leg is limited by the force available from the motors (F_{Max}), as given by (6) where (p) is the number of motors.

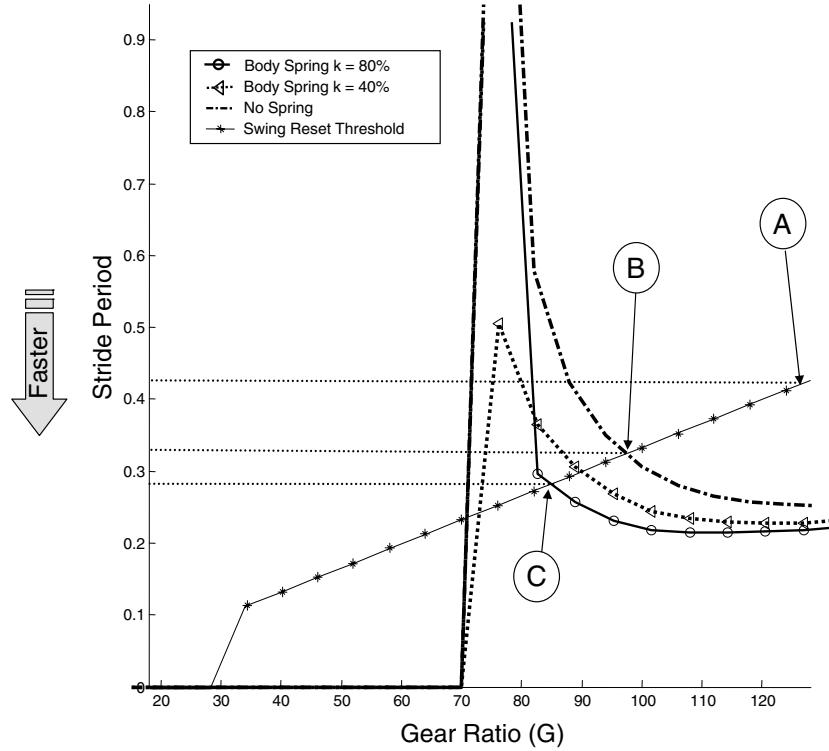


Fig. 7. Simulation results for the model with the body spring. Minimum possible stride periods for various gear ratios (G) and spring constants (k)

$$k \leq \frac{G F_{Max} p}{2R} \quad (6)$$

Magnitudes ranging from 0-80% of the maximum force were evaluated. The simulation results with this spring are shown in Fig. 7.

As in Fig. 5 the areas under the curved lines represent speeds for which the stance phase displacement requirement is not satisfied, and the starred diagonal line represents the swing phase requirement. Points (A) and (B) are the same as in Fig. 5. Point (C) represents the maximum speed with the body spring which yields a 16% improvement over trajectory refinement alone, case (B).

It appears that the use of such a body spring increases the maximum possible speed for a given G , but does not lower the gear ratio which is necessary to overcome gravity and lift the robot. Thus the use of a body spring to some degree duplicates the benefit from implementing a stride-to-stride velocity adaptation scheme.

3.4 Swing-Stance Transfer

A second approach to using springs to more effectively and evenly apply the torque from the motors is to use a spring connecting the foot to the body. As shown on the left in Fig. 8, this is modeled as a spring acting in parallel to the actuator in each virtual leg. This spring is loaded during swing phase as the leg resets to a position relative to the body ready for touch down. The spring is then released at the beginning of stance to assist with the acceleration of the body. As shown on the right in Fig. 8, this adds a load to the motors during swing (when their torque output capabilities are currently underutilized) and mitigates the force requirements at the beginning of stance.

The addition of this spring results in the same body equation of motion as in Sect. 3.3, but the spring is now fully loaded at the beginning of stance, and is fully unloaded at the end. The spring constant, k , is chosen in the same manner as in the previous section.

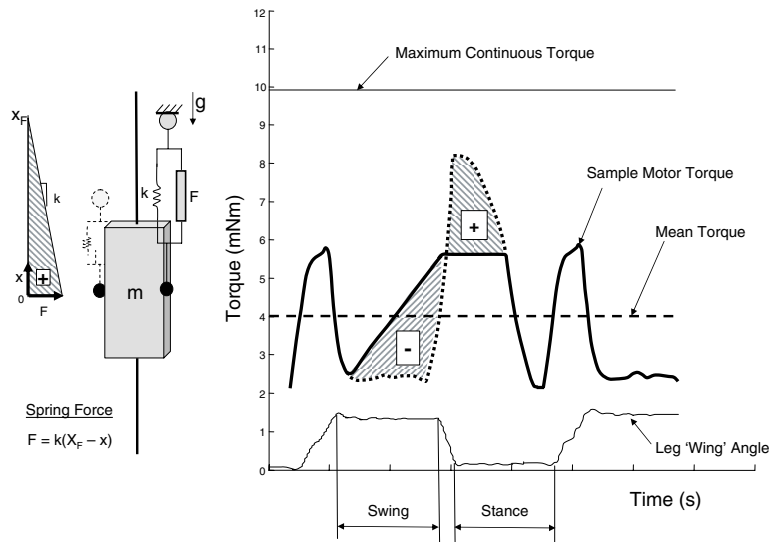


Fig. 8. Schematic of model with leg spring and the effect of the spring on the nominal torque profile. The “+” region represents when the spring is assisting the motor, and the “-” region represents when the motor is stretching the spring. (As before, the leg trajectory and mean torque plots are based on RiSE robot data [3])

Figure 9 shows the effect of changing the gear ratio G on the stride period for a range of spring constants from 0–80% of the maximum spring constant for each G as given by (6). For each value of G and k , the resulting minimum stride period is shown. As before, the line corresponding to the stride period limit for retraction of the leg during swing is indicated with a starred line.

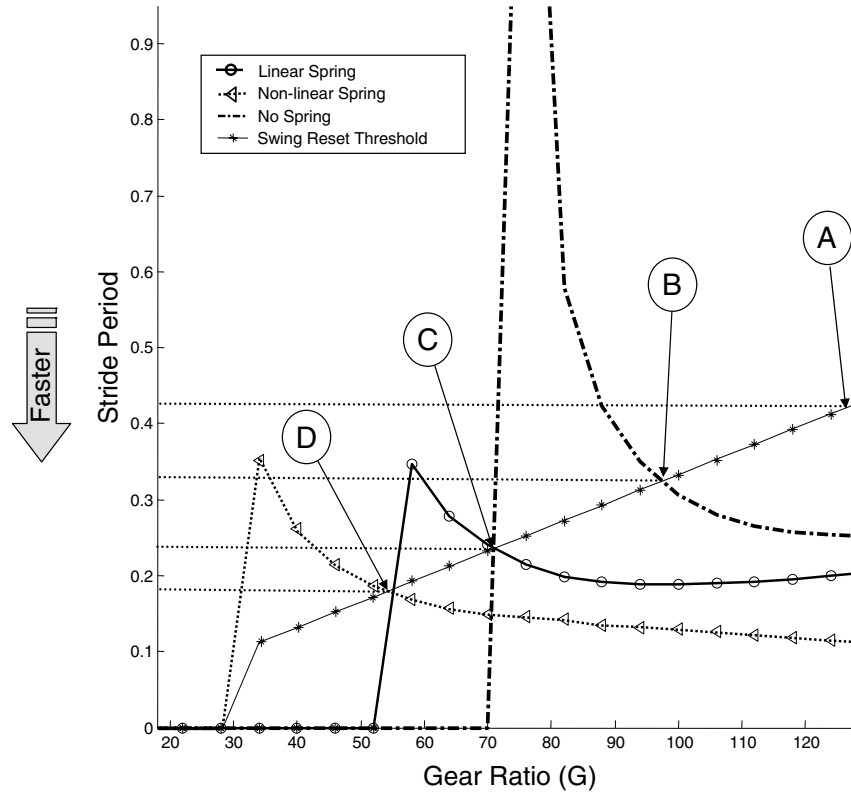


Fig. 9. Simulation results for the model with the leg spring. Minimum possible stride periods for various gear ratios (G) and spring constants (k)

Points (A) and (B) are the same as in Fig. 5 and represent the maximum possible speed without springs. Point (C) indicates the maximum speed configuration for a model with a linear spring with $k = 80\%$ of maximum. The use of a linear spring increases the maximum speed by 36% to 0.62 m/s.

Softening Spring

While advantageous for their simplicity, linear springs are not optimal in terms of energy storage for a limited stretching force. If the linear spring were replaced by a softening spring the spring potential energy at maximum deflection would increase. In the limit, with a constant force spring, the energy storage would double. A constant force spring, however, would add a large load to the beginning of the swing phase when the motors may already be saturated attempting to accelerate the leg. The leg spring analysis in the previous section was repeated with the linear spring replaced by one with a spring equation

of: $F = kx^{\frac{1}{2}}$. This significantly increases the energy storage for the spring with minimal interference with the acceleration of the leg in swing. Point (D) in Fig. 9 represents the fastest configuration that can be achieved with this softening spring, resulting in a speed increase to 0.84 m/s.

Retraction Dynamics

In this swing-to-stance spring approach the load during the swing phase is significantly increased, therefore it becomes important to determine what happens when the leg dynamics are explicitly considered. In other words, at what point will the inertia of the legs and the frictional losses in the springs erode any benefit from running dynamically or adding leg springs.

To this end the dynamics of the swing legs were modeled with (7).

$$\ddot{x}_f = \frac{1}{m_2} \left(\min \left(\frac{G^2 \dot{x}_f - G \dot{x}_{fnl}}{-k_e}, GF_{Max} \right) + k(X_{body} - x_f) - b \dot{x}_f m_2 g \right) \quad (7)$$

Where m_2 is the effective inertia of the robot's leg and b is the damping term, as given by (8).

$$b = 2\zeta\sqrt{mk} \quad (8)$$

While both adding inertia to the legs and increasing the losses in the spring detract from the gains suggested by the simulation, the model can still climb with a spring constant, $k = 80\%$ of maximum, at speeds equivalent to what the simple swing phase model predicts with leg inertias of 30% of the bodymass and a damping coefficient $\zeta = 0.3$.

3.5 Results of Numerical Study

Table 1 summarizes the cases considered thus far and gives the maximum frequency, speed, and percent improvement for each case. With a force-optimization series of trajectory refinements the robot's speed can (theoretically) be significantly improved. Obviously real-world issues associated with mechanical losses and foot attachment/detachment will prevent the actual achievement of the 3.05 Hz theoretical speed predicted from implementing trajectory refinements.

The last row in the table (Combination) shows the effect of combining the body and softening foot springs and allowing the body velocity to increase from stride to stride (momentum), which results in a 2.9x improvement over the trajectory refinement case alone. Even if drag and attachment losses only permitted achieving 40% of the theoretical speed limit, with these changes we get near the 3.5 Hz dynamic threshold that we established previously. Of the various elements, the non-linear foot spring contributes the most.

Another option to improve the speed of the robot climbing is to alter its power/weight ratio. As a point of comparison the motor specs for larger motors

Table 1. Frequency, velocity, and percent improvement for cases (B) to (G)

Case	Frequency	Velocity (m/s)	% Impr.
(A) Trajectory Refinement	3.05	0.46	0
(B) Body Momentum	3.66	0.55	20
(C) Body Spring	3.55	0.53	16
(D) Foot Spring-Linear	4.15	0.62	36
(E) Foot Spring-Softening	5.59	0.84	83
(F) Body + Foot Springs	5.78	0.87	89
(G) Combination	8.85	1.33	190

from the same vendor and product line were used in the model to see how much the power needed to be increased to match the effect of adding springs and dynamic gaits. In this case the 4.5 W motors for RiSE were replaced with 20 W versions. The total mass of the robot was left unchanged and the simulations repeated. This 4.4x increase in power resulted in a 2.3x increase in speed. A net increase slightly less than with springs/dynamics.

In reality the use of larger motors brings with it a significant increase in mass and complexity. The addition of these larger motors would add additional 1.5 kg to the robot’s mass, not including the necessary changes to the body, battery, and electronics design. Fundamentally, increasing the size of the motors does not substantially increase their power to weight ratio. Other motors do have higher power/weight ratios than the ones chosen for our robot, but these suffer from other draw backs such as controllability.

Of course reducing the weight of the robot, were we able to find a way to do it without losing performance, would help as well. The simulations with the simple model described here suggest that gains in speed comparable to the use of springs or the addition of (magically) more powerful motors can be achieved by reducing the robot’s weight by about 50%.

In the absence of further improvements to the power/weight ratio of our robots, the simulations suggest that with our current design it is not possible to reach our target speed. Simply refining the gait and reducing the inefficiencies in the system will, by themselves, be insufficient. With an appropriate use of springs and body dynamics, however, our target speed of 3.5 Hz becomes theoretically possible. The actual realization of these speeds, however, depends on how well these concepts can be incorporated with the ongoing work in improving trajectory refinement and foot attachment.

4 Conclusion

One of the significant problems in achieving fast climbing is the power demand associated with delivering the required work against gravity at higher speeds. Having sufficient on-board power for fast locomotion on the level ground has

proven challenging, and motion against gravity, obviously, only exacerbates the problem. One approach to increasing the use of a robot's onboard power is switch from a position-based control scheme to forced-based approach. By explicitly regulating the motors' output rather than relying on position tracking errors, the actuators can be much more effectively utilized during a stride. This adoption of this control framework also enables the robot to build up speed over a number of strides, further increasing the performance gains.

Even if the switching the fundamental control scheme from a position-based approach proves infeasible (e.g., perhaps because our limited degrees of freedom require intricately planned approaches and departures from stance to guaranteed adequate wall adhesion and limited perturbation during detachment), much of the advantage of a force-based system could be duplicated by very careful trajectory tuning and adaptation.

In either case the refinement of the force trajectory can bring substantial performance benefits to the robot. The simple model employed here suggests that as a theoretical upper limit they could allow the robot to climb at 3Hz or at 0.46 m/s, which is near our dynamic threshold. Of course attachment, detachment and other physical constraints will necessarily reduce the actual gains.

However, in this respect the remainder of the numerical results from the simplified model are encouraging. They suggest that the appropriate addition of body and leg springs could double the robot's speed over this value. The further incorporation of a variable stride period could almost triple the speed over trajectory refinement alone. This is more than the effect of increasing the motor's power 4.4x! (that is of course without acknowledging and accounting for the weight of the larger motors). While the advantages of these approaches are not entirely "free", they do represent a significant gain. When the various refinements are combined, the model results suggest that locomotion at our dynamic threshold of 3.5 Hz (or 2 bodylengths/second) should be achievable.

4.1 Future Work

In order to implement body dynamic dependent gait trajectories some sort of control system to measure body velocity and alter the leg trajectory may be necessary to ensure good attachment of the feet. More detailed foot/substrate interaction tests may provide the empirical data necessary to develop such a controller.

Although we have assumed that foot contact once made will only be broken at the desired detachment point, this clearly does not reflect the reality. Reducing the demands on the foot attachment mechanism could be one of the major advantages of dynamic climbing. It seems possible that an appropriate use of springs and the robot's body's dynamics could significantly reduce the required foot reaction forces. If force threshold limits were added to the feet the effectiveness of the various schemes proposed in this paper could be evaluated in this regard.

Although not addressed here, the stability of dynamic climbers is a topic of interest. Besides the fundamental issues of insuring that the front feet stay attached to the wall, there are a number of other possible ways to consider stability. Many of these arise with the shift from a position-based control to a force-based system. The numeric simulation results suggest that when the velocity is allowed to vary from stride to stride that the simple climber tends to quickly converge to a steady period-1 gait. Have we been fortuitous in our parameter selection, or are these limit cycles almost inevitable? Are they local in nature hence hard to achieve in practice or do they have large basins (e.g., are they globally asymptotic stable)? The model we have used may be simple enough to permit a careful mathematical analysis of the system dynamics.

A second interesting question that arises from decoupling multiple limbs from a trajectory-tracking control scheme is the question of synchronization. A related climbing study with an open-loop climbing model [17] indicates that legs tend to synchronize rather than staying 180 degrees out of phase. Is this also true for this model, and if so what sort of controller needs to be established to maintain a regular alternating gait?

Looking further ahead, we wonder if with the addition of a lateral degree of freedom to the model we can begin to duplicate the motions and ground reaction forces seen in dynamic climbing animals such as geckos and cockroaches.

We believe that enabling a robot with the ability to both dynamically run and climb is an compelling goal. The achievement of both with an (inherently) constrained power/weight ratio is a difficult task. The creative use of springs and system dynamics to modify the climbing motion of the robot may enable the construction of such robots. While we are not there yet, we at least have some simple models that suggest that it may be possible.

Acknowledgments

Thanks to RiSE team for many stimulating conversations, specifically: Ron Fearing, Martin Buehler for their thoughts on motors and power in climbing, Jonathan Karpick for ideas about how to use dynamics in climbing, Dan Goldman, for discussions about how biological systems climb, and Haldun Kom-suoglu for insights about modeling simple climbers. We also appreciate Clark Haynes and Al Rizzi's help with the robot trajectory and power consumption data. The development of the RiSE platform was supported by DARPA under grant number N66001-05-C-8025. Jonathan Clark is supported by the DCI Postdoctoral Fellow Program under grant number HM158204-1-2030.

Appendix A1: Rise Robot Constants

Appendix A2: Minimum Leg Frequency

In order to achieve resonant hopping as described by the spring-loaded inverted pendulum (SLIP) model, the motor activation frequency—whether used primarily for recirculating vertical leg springs as in RHex [6] or for powering vertical leg strokes in phase with passive recirculating springs as in Sprawl [14]—should match the natural frequency of the body’s oscillation. For a SLIP-type hopper the natural frequency, ω_n , during stance is a function of the body mass, M , and stiffness of the legs, k , that varies in a rather subtle manner with the particular steady state gait for even the simplest two degree of freedom models [5]. Empirically, we find this function is effectively approximated by that characterizing a one degree of freedom spring-mass system:

$$\omega_n = \sqrt{\frac{k}{M}} \quad (9)$$

The lower limit on the spring stiffness is constrained by its maximum displacement, Δx , which in turn is fixed by the leg kinematics. Although the force-extension profile of a spring can vary significantly depending upon whether it is “hardening” or “softening”, it will suffice for our present order-of-magnitude analysis to consider the simplest relationship of constant stiffness arising from a Hooke’s law spring. For this model, a lower bound on the excursion of the leg spring corresponds to when the force on the spring is equal to gravity, giving:

$$k = \frac{Mg}{\Delta x} \quad (10)$$

Combining equations (9) and (10) gives:

$$\omega_n = \sqrt{\frac{k}{M}} = \sqrt{\frac{Mg}{\Delta x M}} = \sqrt{\frac{g}{\Delta x}}$$

For RiSE with a kinematically achievable $\Delta x = 0.02$ m:

Table 2. RiSE specific model parameter values

Variable	Value	Description
T_{Stall}	0.0288 Nm	Stall torque
T_{Max}	0.00498 Nm	Maximum continuous torque
ω_{nl}	13,900 rpm	No-load speed
R	0.0762 m	Radius of foot trajectory
G	126	Base Gear ration
p	6	Number of motors per tripod
m	3 kg	Mass of the robot

$$\omega_n = 22 \text{ rad/s} = 3.5 \text{ cycles/s}$$

If large airborne phases are allowed the body oscillation frequency would become slower than the body spring-mass frequency, ω_n . Any gains from this, however, would be set off by the increased required deflection of the spring, Δx , during stance.

References

- [1] <http://www.vortexhc.com/vmrp.html>.
- [2] <http://www.maxonmotorusa.com>.
- [3] Personal Communication from Al Rizzi and Clark Haynes.
- [4] R. McN. Alexander. Mechanics and scaling of terrestrial locomotion. In T. J. Pedley, editor, *Scale Effects in Animal Locomotion*, pp. 93–110. Academic Press, 1977.
- [5] R. Altendorfer, D. E. Koditschek, and P. Holmes. Stability analysis of legged locomotion models by symmetry-factored return maps. *International Journal of Robotics Research*, 23(11):979–1000, 2004.
- [6] R. Altendorfer, N. Moore, H. Komsuoglu, M. Buehler, Jr. Brown H. B, D. McMordie, U. Saranli, R. Full, and D. E. Koditschek. Rhex: A biologically inspired hexapod runner. *Autonomous Robots*, 11(3):207–213, 2001.
- [7] A. T. Asbeck, S. Kim, W. R. Provancher, M. R. Cutkosky, and M. Lanzetta. Scaling hard vertical surfaces with compliant microspine arrays. In *Proceedings, Robotics Science and Systems Conf., MIT, Cambridge, MA, June 8–10, 2005*.
- [8] K. Autumn, M. Buehler, M. Cutkosky, R. Fearing, R. J. Full, D. Goldman, R. Groff, W. Provancher, A. A. Rizzi, U. Saranli, A. Saunders, and D. E. Koditschek. Robotics in scansorial environments. In Grant R. Gerhart, Charles M. Shoemaker, and Douglas W. Gage, editors, *Unmanned Ground Vehicle Technology VII*, vol. 5804, pp. 291–302. SPIE, 2005.
- [9] K. Autumn, S. T. Hsieh, D. M. Dudek, J. Chen, Chitaphan. C., and R. J. Full. Dynamics of geckos running vertically. 2005. in press.
- [10] C. Balaguer, A. Gimenez, J. M. Pastor, V. M. Padron, and C. Abderrahim. A climbing autonomous robot for inspection applications in 3d complex environments. *Robotica*, 18:287–297, 2000.
- [11] D. Bevly, S. Dubowsky, and C. Mavroidis. A simplified cartesian-computed torque controller for highly geared systems and its application to an experimental climbing robot. *Transactions of the ASME. Journal of Dynamic Systems, Measurement and Control*, 122(1):27–32, 2000.
- [12] T. Bretl, S. Rock, and J. C. Latombe. Motion planning for a three-limbed climbing robot in vertical natural terrain. In *Proceedings of the IEEE International Conference on Robotics and Automation*, vol. 205, pp. 2946–2953. Piscataway, NJ, USA: IEEE, 2003.
- [13] G. A. Cavagna, N. C. Heglund, and Taylor C. R. Mechanical work in terrestrial locomotion: Two basic mechanisms for minimizing energy expenditure. *American Journal of Physiology*, 233, 1977.
- [14] J. G. Cham, S. A. Bailey, J. E. Clark, R. J. Full, and M. R. Cutkosky. Fast and robust: Hexapedal robots via shape deposition manufacturing. *International Journal of Robotics Research*, 21(10), 2002.

- [15] J. G. Cham, J. Karpick, J. E. Clark, and M. R. Cutkosky. Stride period adaptation for a biomimetic running hexapod. In *International Symposium of Robotics Research*, Lorne Victoria, Australia, 2001.
- [16] S. Kim, A. Asbeck, M. R. Cutkosky, and W. R. Provancher. Spinybotii: Climbing hard walls with compliant microspines. In *Proceedings, IEEE – ICAR, Seattle, WA, July 17–20, 2005*.
- [17] Haldun Komsuoglu. *Toward a formal framework for open-loop stabilization of rhythmic tasks*. PhD thesis, University of Michigan, 2004.
- [18] R. Kram, A. Domingo, and D. P. Ferris. Effect of reduced gravity on the preferred walk-run transition speed. *The Journal of Experimental Biology*, 200:821–826, 1991.
- [19] G. La Rosa, M. Messina, G. Muscato, and R. Sinatra. A low-cost lightweight climbing robot for the inspection of vertical surfaces. *Mechatronics*, 12(1):71–96, 2002.
- [20] T. A. McMahon and G. C. Cheng. Mechanics of running. how does stiffness couple with speed? *Journal of Biomechanics*, 23(1):65–78, 1990.
- [21] R. D. Quinn, G. M. Nelson, R. J. Bachmann, D. A. Kingsley, J. Offi, and R. E. Ritzmann. Insect designs for improved robot mobility. In Dillmann Berns, editor, *Proceedings of CLAWAR 2001, Karlsruhe, Germany*, pp. 69–76, 2001.
- [22] M. Sitti and R. S. Fearing. Synthetic gecko foot-hair micro/nano-structures for future wall-climbing robots. In *Proceedings of the IEEE International Conference on Robotics and Automation*, vol. 1, pp. 1164–1170. Piscataway, NJ, USA: IEEE, 2003.
- [23] Z. L. Xu and P. S. Ma. A wall-climbing robot for labelling scale of oil tank’s volume. *Robotica*, 20:209–212, 2002.